Synthesis and photophysics of new pyridyl end-capped 3D-dithia[3.3]paracyclophane-based Janus tectons: surface-confined self-assembly of their model pedestal on HOPG

M Auffray, F. Charra, L Sosa Vargas, F. Mathevet, André-Jean Attias, David Kreher

HAL Id: hal-02879945

https://hal.sorbonne-universite.fr/hal-02879945

Submitted on 24 Jun 2020

NJC

ARTICLE

Synthesis and photophysics of new pyridyl end-capped 3D-dithia[3.3]paracyclophane-based Janus tectons: surface-confined self-assembly of their model pedestal on HOPG

M. Auffray,[a] F. Charra, [b] L. Sosa Vargas,[a] F. Mathevet,[a] A-J. Attias [a] and D. Kreher [a*]

Surface-confined supramolecular self-assembly is currently a promising strategy to create well-organised 2D-networks on conducting surfaces. However, using such substrates tends to quench any electronic properties of the adsorbed molecules. In this context, new pyridyl end-capped 3D-dithia[3.3]paracyclophane-based molecules were designed, as well as its model compound (pedestal), with the objective of self-assembling these tectons on any substrate. The synthesis of these new molecules was not straightforward and is consequently described into detail. Once the materials were successfully isolated, their optoelectronic properties were investigated to study potential non-covalent interactions: by pH-dependant absorption and emission measurements, and by infra-red spectrometry. We evidenced that both ionic and coordination bonding are compatible with the molecules' design. Finally, preliminary scanning tunneling microscopy (STM) studies were performed to study the supramolecular self-assembly properties of the model lower-deck (pedestal) on highly oriented pyrollitic graphite (HOPG): we observed a quasi-square lattice of self-assembled 2D-networks which appear to form independently of the underlying HOPG lattice.

1. Introduction

In the field of nanotechnology, surface science plays a crucial role as most (nano-) devices eventually need to be supported on a surface. Therefore, controlling the adsorption on surface is utterly required, and commonly two contrasting strategies can be cited: top-down and bottom-up approaches.[1] This latter consists in creating from a substrate a macro-scale object, starting from specifically designed molecular building blocks (tectons), through either chemisorption or physisorption process. In particular, the physisorption strategy is entirely based on the spontaneous organisation of molecules into stable and structurally well-defined networks on the surface, occurring by reversible supramolecular bonds between molecules and substrates, also called supramolecular self-assembly. On the one hand, the supramolecular bond between molecule and substrate depends on the nature of both, for example, the van der Waals interactions between alkyl chains and highly oriented pyrolytic graphite (HOPG).[2] On the other hand, it can be tuned *via* the main interactions between molecules themselves. In this context, surface-confined self-assembly at the liquid/solid interface is considered nowadays as a promising approach for directly building low-dimensional (2D) supramolecular nanostructures on surfaces, under

both dynamic and thermodynamic control.[3] Several examples have already been developed, by exploiting various supramolecular interactions such as van der Waals interactions,[4] ionic bonds,[5] hydrogen bonds,[6] halogen bonds[7] or even coordination.[8] But in view of practical applications, it is still challenging to obtain functional surfaces, in particular due to the fact that by using semi-conducting or conducting substrates, charge-transfer and hybridisation occurring between the molecules and the substrate might significantly alter the electronic properties of the adsorbed molecules. As a consequence, and to preserve the electronic properties, the molecule has to be decoupled (or "lifted") from the substrate.[9] To overcome this issue, effective ways of decoupling have been studied by using multilayers of molecules,[10] ultra-thin insulating layers onto the conducting surface[11] or by chemically modifying the structure molecule with molecular landers.[12]

However, all these strategies do not allow to preserve simultaneously both the self-assembly and the electronic properties of the adsorbed molecules. Moreover, drastic conditions such as low temperature and high vacuum are required. To overcome this drawback, our group recently proposed a new molecular design strategy that will allow us to conserve the molecular electronic properties whilst maintaining a stable, supramolecular self-assembled network. Our goal was to achieve a highly ordered, self-assembly on highly oriented pyrolytic graphite (HOPG) and graphene substrates at room temperature, by using the so-called Janus-like 3D-tecton design.[13] This type of molecular architecture presents doubly-functionalised building blocks where two opposite faces are linked

a. *Sorbonne Université, UPMC Univ Paris 06, Institut Parisien de Chimie Moléculaire, UMR CNRS 8232, 4 Place Jussieu, 75252 Paris Cedex 05, France.*
b. *Service de Physique de l'Etat Condensé, CEA CNRS Université Paris-Saclay, CEA Saclay, F-91191 Gif-sur-Yvette Cedex, France.*

by a rigid dithia[3,3]paracyclophane bridge. One face (pedestal) is responsible for guiding the 2D self-assembly whereas the other can be functionalised at will by any active moiety. The concept was proven successful, and the fluorescence of self-assembled molecular monolayers could be measured from perylene-functionalised Janus tectons on graphene, at ambient conditions.[14] These Janus-tectons were initially developed with self-organising pedestals that were driven by van der Waals interactions between alkylated chains.

But such a design restricted its adsorption to only sp^2-hybridised carbon substrates as HOPG or graphene. Therefore, a new design of cyclophane-based molecules is proposed using a new pedestal able to adsorb and self-organise on any substrate, by exploiting different supramolecular interactions. To achieve this goal, the pyridine moiety was chosen due to its well-known ability to form ionic bonds *via* a simple protonation, halogen or hydrogen bonding or coordination-type bonding with the corresponding additives.[15]

2. Experimental

2.1 Materials and methods

All solvents and reactants were purchased from commercial suppliers. The reactants were used without further purification. When necessary, the solvents were dried by using a MBraun solvent purification system (MB SPS-800). The organic compounds purifications performed by chromatography were either carried out by gravity column chromatography using silica gel (Si 60, 40-63 μm, Merck) or by flash chromatography (Combiflash Companion) with the same type of silica. The nuclear magnetic resonance experiments were recorded at 300 or 600 MHz (Bruker, BBFO probe for the 2D-experiments). The proton and carbon chemical shifts (δ) are reported in ppm and are referenced to the residual solvent signal: chloroform ($CDCl_3$, 7.26, 77.16). Infra-red spectra were recorded with a ThermoFisher Nicolet iS10 FT-IR spectrometer. UV/Vis spectra were recorded with a Varian Cary WinUV spectrophotometer. The cells were in quartz with two faces (thickness: 1cm). Photoluminescence spectra were recorded with a Varian Cary Eclipse fluorescence spectrophotometer. STM images were acquired at room temperature with a homemade digital system. The fast scan axis was kept perpendicular to the sample slope. Images acquired simultaneously in both fast scan directions are systematically recorded and compared. All images are corrected for the drift of the instrument by combining two successive images with downward and upward slow-scan directions. The solvent was phenyloctane (Aldrich, 98%). The substrate was HOPG (Goodfellow) and the tips were mechanically formed from a 250mm Pt–Ir wire (Pt80/Ir20, Goodfellow). The monolayers were formed by drop casting a droplet (ca. 10 μL, in dichloromethane) of the solution immediately after cleaving the substrate. The samples were heated at 80°C for 10 minutes before immersing the STM junction in an additional droplet of phenyloctane (ca. 10 μL) and approaching the STM tip.

2.2 Synthesis

Synthesis of 1,4-Bis[(trimethylsilyl)ethynyl]-2,5-dimethylbenzene 1.[16] In a Schlenk tube, 2,5-dibromo-*p*-xylene (2 g, 7.6 mmol), $PdCl_2(PPh_3)_2$ (265 mg, 0.4 mmol), copper(I) iodide (70mg, 0.4 mmol) and triethylamine (40 mL, 300 mmol) were added and put undert an Argon atmosphere. Trimethylsilylacetylene (3.5 mL, 24 mmol) wasadded, and the Schlenk tube was sealed. The mixture was stirred at 100°C for 8 hours. The solution was diluted with dichloromethane, washed with water and dried over magnesium sulfate. After evaporation *in vacuo*, the residue was purified by flash chromatography (SiO_2, petroleum ether) to afford **1** as a white powder in 91 % yield. ^1H NMR (300 MHz, $CDCl_3$) δ 7.26 (s, 2H), 2.34 (s, 6H), 0.25 (s, 18 H). ^{13}C NMR (300 MHz, $CDCl_3$) δ 137.66, 132.97, 123.18, 104.03, 99.67, 19.97, 0.18.

Synthesis of 1,4-Diethynyl-2,5-dimethylbenzene 2.[17] To a solution of **1** (415 mg, 1.4 mmol) in methanol (25 mL), potassium fluoride (350 mg, 6.0 mmol) was added. The mixture was stirred overnight at room temperature and then evaporated *in vacuo.* The crude product was purified by flash chromatography (SiO_2, dichloromethane) to afford **2** as a light yellow powder in 96 % yield. ^1H NMR (300 MHz, $CDCl_3$) δ 7.26 (s, 2H), 3.33 (s, 2H), 2.34 (s, 6H). ^{13}C NMR (300 MHz, $CDCl_3$) δ 137.91, 133.40, 122.48, 82.33, 82.26, 19.94.

Synthesis of 1,4-Bis[(pyridyl)ethynyl]-2,5-dimethylbenzene P.[18] In a Schlenk tube, compound **2** (200 mg, 1.3 mmol), *p*-bromopyridine hydrochloride (500 mg, 2.0 mmol), $Pd(PPh_3)_2Cl_2$ (46 mg, 0.07 mmol) and CuI (13 mg, 0.07 mmol) were introduced. Then, diisopropylamine (15 mL, 107.0 mmol) was added and the mixture was stirred at RT, under an argon atmosphere for 8 hours. The resulting solution was diluted with dichloromethane, washed with water and dried over magnesium sulfate. After evaporation *in vacuo*, the residue was purified by flash chromatography (SiO_2, petroleum ether/ethyl acetate, 9:1) to afford **P** as a white powder in 85 % yield. ^1H NMR (300 MHz, $CDCl_3$) δ 8.63 (m, 4H), 7.40 (m, 6H), 2.49 (s, 6H). ^{13}C NMR (300 MHz, $CDCl_3$) δ 149.89, 138.03, 133.26, 131.59, 125.59, 122.92, 92.75, 92.18, 20.12. HRMS: (EI) m/z (%) for C22H16N2; calcd 308.1313; found 308.1315. Anal. Calcd for C22H16N2 (MW 308.13): C, 85.69; H, 5.23; N, 9.08. Found: C, 85.75; H, 5.29; N, 8.92.

Synthesis of 1,4-dibromo-2,5-bis(bromomethyl)benzene 3.[19] To a solution of 2,5-dibromo-*p*-xylene (5 g, 19 mmol) in acetonitrile (75 mL) NBS (7.1 g, 40 mmol) and AIBN (160 mg, 1 mmol) were added. The mixture was left stirring for 24 hours under reflux, after which the mixture was evaporated *in vacuo* and washed by hot methanol to afford **3** as a white powder in 60% yield. Mp = 161°C. ^1H NMR (300 MHz, $CDCl_3$) δ 7.66 (s, 2H), 4.51 (s, 4H). ^{13}C NMR (300MHz, $CDCl_3$) δ 139.14, 135.50, 123.43, 31.62.

Synthesis of 1,4-dibromo-2,5-dimethoxymethylbenzene 4. In a Schlenk tube compound **3** (1 g, 2.4 mmol), was added to degassed methanol (20 mL) and set to stir under an argon atmosphere. After stirring for 10 minutes, a freshly prepared sodium methoxide (0.14 g of sodium in 20 mL of methanol) was added dropwise. Upon addition, the reaction was heated to 90°C and left stirring overnight. The resulting solution was then poured into water, extracted with dichloromethane and dried over magnesium sulfate. The

dichloromethane was removed *in vacuo* to afford the *title compound* **4** as a white powder in quantitative yield. Mp = 70°C. ^{1}H NMR (300 MHz, CDCl$_3$) δ 7.63 (s, 2H), 4.47 (s, 4H), 3.47 (s, 6H). ^{13}C NMR (300 MHz, CDCl$_3$) δ 138.50, 112.33, 121.30, 73.23, 58.89.

Synthesis of 1,4-bis[(trimethylsilyl)ethynyl]-2,5-dimethoxymethyl benzene 5. In a Schlenk tube, compound **4** (1.9g, 6 mmol), PdCl$_2$(PPh$_3$)$_2$ (200 mg, 0.3 mmol), CuI (0.1 mg, 0.3 mmol) and triethylamine (30 mL, 225 mmol) were mixed together under an argon atmosphere. Trimethylsilylacetylene (2.7 mL, 19 mmol) was then added, the Schlenk tube was sealed and the mixture stirred at 100°C for 8 hours. The resulting solution was diluted with dichloromethane, washed with water and dried over magnesium sulfate. After evaporation *in vacuo*, the residue was purified by flash chromatography (SiO$_2$, petroleum ether) to afford the *title compound* **5** as a white powder in 84 % yield. Mp = 89 °C. ^{1}H NMR (300 MHz, CDCl$_3$) δ 7.53 (s, 2H), 4.57 (s, 4H), 3.44 (s, 6H), 0.24 (s, 18H).. ^{13}C NMR (300 MHz, CDCl$_3$) δ 139.43, 121.23, 122.01, 100.96, 72.11, 58.73, 0.07.

Synthesis of 1,4-diethynyl-2,5-bis(bromomethyl)benzene 6.[20] In a Schlenk tube compound **5** (0.45g, 1.2 mmol) and dichloromethane (10 mL) were introduced and placed under an argon atmosphere. The mixture was then cooled to 0°C and then left to stir for 10 minutes, after which a solution of BBr$_3$ (3.7 mL, 3.7 mmol) in dichloromethane (10 mL) was added dropwise through a dropping funnel. After stirring for 2 hours, the reaction mixture was poured into water and extracted with dichloromethane. The solution was dried over magnesium sulfate and evaporated *in vacuo*. The crude mixture obtained was then dissolved in methanol (80 mL) and potassium fluoride (340 mg, 6 mmol) was added. The solution was stirred overnight at room temperature and then poured onto water, extracted with dichloromethane and dried over magnesium sulfate. The solution was then evaporated *in vacuo* to afford the *title compound* **6** as a light-yellow powder in 47% yield. ^{1}H NMR (300 MHz, CDCl$_3$) δ 7.58 (s, 2H), 4.60 (s, 4H), 3.51 (s, 2H). ^{13}C NMR (300 MHz, CDCl$_3$) δ 140.13, 134.50, 122.98, 85.02, 79.83, 30.15.

Synthesis of 4'-bromo-2,5-dimethyl-1,1'-biphenyl 7. *p*-bromo-phenyl boronic acid (860 mg, 4.30 mmol) and Pd(PPh$_3$)$_2$Cl$_2$ (175 mg, 0.25 mmol) were added to a solution of 2-iodo-*p*-xylene (0.62 mL, 4.30 mmol) in dioxane (20 mL) in an argon atmosphere. Then, K$_2$CO$_3$ (2 g, 15.00 mmol) dissolved in water (5 mL) was added, and the mixture was heated at 110°C for 12 hours. The reaction was cooled to room temperature, and washed with water. The mixture was then extracted with dichloromethane, dried over magnesium sulfate and evaporated *in vacuo*. The crude was purified by chromatography (SiO$_2$, petroleum ether) to afford the *title compound* **7** as a colourless oil in 94% yield. ^{1}H NMR (300 MHz, CDCl$_3$) δ 7.61 (d, [3]J = 8.5 Hz, 2H), 7.27 (d, [3]J = 8.5 Hz, 2H), 7.25 (d, [3]J = 8.0 Hz, 1H), 7.18 (d, [3]J = 8.0 Hz, 1H), 7.12 (s, 1H), 2.45 (s, 3H), 2.31 (s, 3H). ^{13}C NMR (300 MHz, CDCl$_3$) δ 141.05, 140.56, 135.40, 132.07, 131.26, 130.95, 130.49, 130.38, 128.40, 130.98, 21.01, 20.00.

Synthesis of 1,4-bis(bromomethyl)benzene 8a. [18] NBS (7.1 g, 40 mmol) and AIBN (160 mg, 1 mmol) were added to a solution of *p*-xylene (2 g, 19 mmol) in acetonitrile (60 mL). After stirring for 16 hours under reflux, the mixture was evaporated *in vacuo* and purified by flash chromatography (SiO$_2$, petroleum ether: dichloromethane 1:1) to afford **8a** as a white powder in 87% yield. ^{1}H NMR (300 MHz, CDCl$_3$) δ 7.37 (s, 4H), 4.48 (s, 4H).

Synthesis of the 4'-bromo-2,5-bis(bromomethyl)-1,1'-biphenyl 8b. To a solution of **7** (1 g, 3.8 mmol) in acetonitrile (100 mL) NBS (1.4 g, 8,0 mmol) and AIBN (60 mg, 0.4 mmol) were added. After stirring for 14 hours at 90 °C, the mixture was evaporated *in vacuo* and purified by flash chromatography (SiO$_2$, Petroleum ether) to afford the *title compound* **8b** as a white powder in 90% yield. ^{1}H NMR (300 MHz, CDCl$_3$) δ 7.60 (d, [3]J = 8.5 Hz, 2H), 7.50 (d, [3]J = 8.0 Hz, 1H), 7.41 (dd, [3]J = 8.0 Hz, [4]J = 2.0 Hz, 1H), 7.32 (d, [3]J = 8.5 Hz, 2H), 7.24 (d, [4]J = 2.0 Hz, 1H), 4.49 (s, 2H), 4.39 (s, 2H).

Synthesis of the 1,4-bis(mercaptomethyl)benzene 9a.[21] To a solution of **8a** (5 g, 18.9 mmol) in ethanol (75 mL) thiourea (3.6 g, 47.4 mmol) was added. The mixture was heated at 80°C for 3h and then cool down to room temperature. After evaporation *in vacuo*, the residue was dissolved in water (20 mL). Sodium hydroxide was added (2.25 g, 56.7 mmol) to the mixture, heated to 100 °C and left overnight. The solution was then extracted with diethylether and dried over magnesium sulfate. Evaporation *in vacuo* gave **9a** as colourless crystals in 79% yield. ^{1}H NMR (300 MHz, CDCl$_3$) δ 7.27 (s, 2H), 3.72 (d, 4H), 1.75 (t, 2H). ^{13}C NMR (300 MHz, CDCl$_3$) δ 140.07, 128.46, 28.72.

Synthesis of the 4'-bromo-2,5-bis(mercaptomethyl)-1,1'-biphenyl 9b. To a solution of **8b** (900 mg, 2.15 mmol) in ethanol (50 mL) thiourea (410 mg, 5.35 mmol) was added. The mixture was heated at 80°C in a sealed Schlenk tube under an argon atmosphere for 3h and then cooled down to room temperature. After evaporation *in vacuo*, the residue was dissolved in water (50 mL) and the solution was degassed. Potassium hydroxide was added (1.2 g, 21.5 mmol) and the mixture was heated at 100 °C overnight in a sealed Schlenk tube. The solution was then extracted with diethylether and dried over magnesium sulfate. The evaporation *in vacuo* gave the *title compound* **9b** as colourless crystals in 83% yield. ^{1}H NMR (300 MHz, CDCl$_3$) δ 7.55 (d, [3]J = 8.5 Hz, 2H), 7.37 (d, [3]J = 8.0 Hz, 1H), 7.29 (dd, [3]J = 8.0 Hz, [4]J = 2.0 Hz, 1H), 7.32 (d, [3]J = 8.5 Hz, 2H), 7.13 (d, [4]J = 2.0 Hz, 1H), 3.72 (d, [3]J = 7.5 Hz, 2H), 3.62 (d, [3]J = 7.5 Hz, 2H), 1.77 (d, [3]J = 7.5 Hz, 1H), 1.66 (d, [3]J = 7.5 Hz, 1H).

Synthesis of the 5,8-diethynyl-2,11-dithia[3.3]paracyclophane 10a. To a solution of potassium hydroxide (100 mg, 1.8 mmol) in methanol (350 mL), a mixture of **6** (400 mg, 1.3 mmol) and **9a** (200 mg, 1.3 mmol) in dichloromethane (50 mL) were added dropwise using a syringe pump (4 mL/h), simultaneously with another solution of potassium hydroxide (200 mg, 3.6 mmol) in methanol (50 mL). At the end of the addition, the mixture was evaporated *in vacuo.* The residue was then dissolved in dichloromethane, washed with water, dried over magnesium sulfate and evaporated again *in vacuo*. The crude was purified by column chromatography (SiO$_2$, petroleum ether: dichloromethane 1:1) to afford the *title compound* **10a** as a white powder in 43 % yield. ^{1}H NMR (300 MHz, CDCl$_3$) δ 7.14 (s, 2H),

7.06 (d, ^3J = 8 Hz, 2H), 7.02 (d, ^3J = 8 Hz, 2H), 4.30 (d, ^3J = 15 Hz, 2H), 3.87 (d, ^3J = 15 Hz, 2H), 3.78 (d, ^3J = 15 Hz, 2H), 3.59 (d, ^3J = 15 Hz, 2H), 3.43 (s, 2H).

Synthesis of the 5,8-diethynyl-13-(*p*-bromophenyl)-2,11-dithia[3.3] paracyclophane 10b. To a solution of potassium hydroxide (100 mg, 1.8 mmol) in methanol (600 mL), a solution of **6** (420 mg, 0.9 mmol) and **9b** (300 mg, 0.9 mmol) in dichloromethane (50 mL) were added dropwise using a syringe pump (3.5 mL/h), simultaneously with another solution of potassium hydroxide (200 mg, 3.7 mmol) in methanol (50 mL). After addition was completed, the mixture was acidified with dilute H_2SO_4, extracted with dichloromethane, washed with water, dried over magnesium sulfate and evaporated *in vacuo*. The crude was purified by flash chromatography (SiO$_2$, petroleum ether: dichloromethane using a gradient from 1:0 to 1:1) to afford the *title compound* **10b** as a white powder with a yield of 60 %. ^{1}H NMR (300 MHz, CDCl$_3$) δ 7.63-7.00 (m, 18H), 4.45-3.46 (m, 16H+4H).

Synthesis of the 5,8-bis[(pyridyl)ethynyl]-2,11-dithia[3.3]para cyclophane C. In a Schlenk tube, **10a** (150 mg, 0.5 mmol), iodopyridine (480 mg, 2.4 mmol), Pd(PPh$_3$)$_2$Cl$_2$ (35 mg, 0.05 mmol) and poper(I) iodide (10 mg, 0.05 mmol) were added under an argon atmosphere. Then, diisopropylamine (1.5 mL, 10.0 mmol) was added and the mixture was stirred for 20 hours at 20°C. The solution was diluted with dichloromethane, washed with water and dried over magnesium sulfate. After evaporation *in vacuo*, the residue was purified by flash chromatography (SiO$_2$, petroleum ether: ethyl acetate, with a gradient 9:1 to 1:1) to afford the *title compound* **C** as a yellow powder in 44 % yield. ^{1}H NMR (300 MHz, CDCl$_3$) δ 8.69 (s, 4H), 7.49 (d, ^3J = 5.5 Hz, 4H), 7.22 (s, 2H), 7.08 (d, ^3J = 8 Hz, 2H), 7.05 (d, ^3J = 8 Hz, 2H), 4.32 (d, ^3J = 15 Hz, 2H), 3.90 (d, ^3J = 15 Hz, 2H), 3.85 (d, ^3J = 15 Hz, 2H), 3.72 (d, ^3J = 15 Hz, 2H). HRMS: (EI) m/z (%) for C$_{30}$H$_{22}$N$_2$S$_2$; calcd 474.1224; found 474.1224.

Synthesis of the 5,8-bis[(pyridyl)ethynyl]-13-(*p*-bromophenyl)-2,11-dithia[3.3]paracyclophane JT. In a Schlenk tube, **10b** (170 mg, 0.36 mmol), iodopyridine (370 mg, 1.8 mmol), Pd(PPh$_3$)$_2$Cl$_2$ (30 mg, 0.04 mmol) and copper iodide(8 mg, 0.04 mmol) were introduced under an argon atmosphere. Diisopropylamine (1,5 mL, 10.0 mmol) was then added and the mixture was stirred for 24 hours at 20°C. The solution was diluted with dichloromethane, washed with water and dried over magnesium sulfate. After evaporation *in vacuo*, the residue was purified by flash chromatography (SiO$_2$, petroleum ether: ethyl acetate, 9:1 to 1:1) to afford the *title compound* **JT** as a yellow powder in 84 % yield. ^{1}H NMR (300 MHz, CDCl$_3$) δ 8.78-8.65 (m, 8H), 7.61-7.06 (m, 26H), 4.45-3.46 (m, 16H). HRMS: (EI) m/z (%) for C$_{36}$H$_{25}$N$_2$S$_2$; calcd 628.0643; found 628.0642.

3. Results and discussion

In this paper, three bis(pyridyl)acetylene derivatives were synthesized (scheme 1): the planar pedestal **P** (for reference), the pedestal incorporating a cyclophane **C** (to check the influence of the cyclophane incorporation) and finally a functionalisable Janus tecton **JT** (where any active component could potentially be grafted).
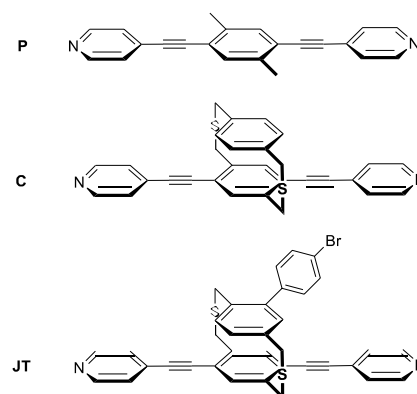
Scheme 1: Bis(pyridyl)acetylene-based target molecules

3.1 Synthesis

The molecule **P** was synthesised from the 2,5-dibromo-*p*-xylene *via* a Sonogashira cross-coupling reaction with trimethylsilylacetylene (TMSA), followed by the deprotection of the trimethylsilyl groups with potassium fluoride and finally by a second Sonogashira coupling with an overall yield of 70% (scheme 2).
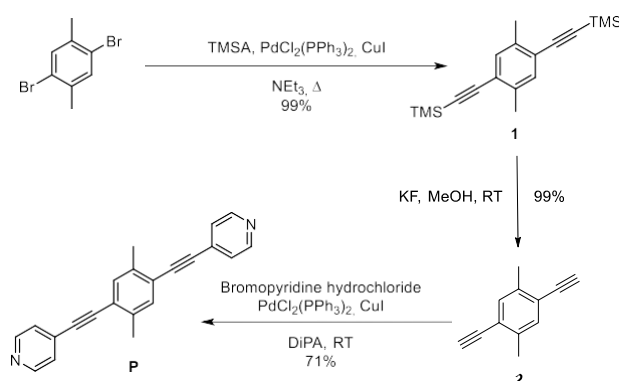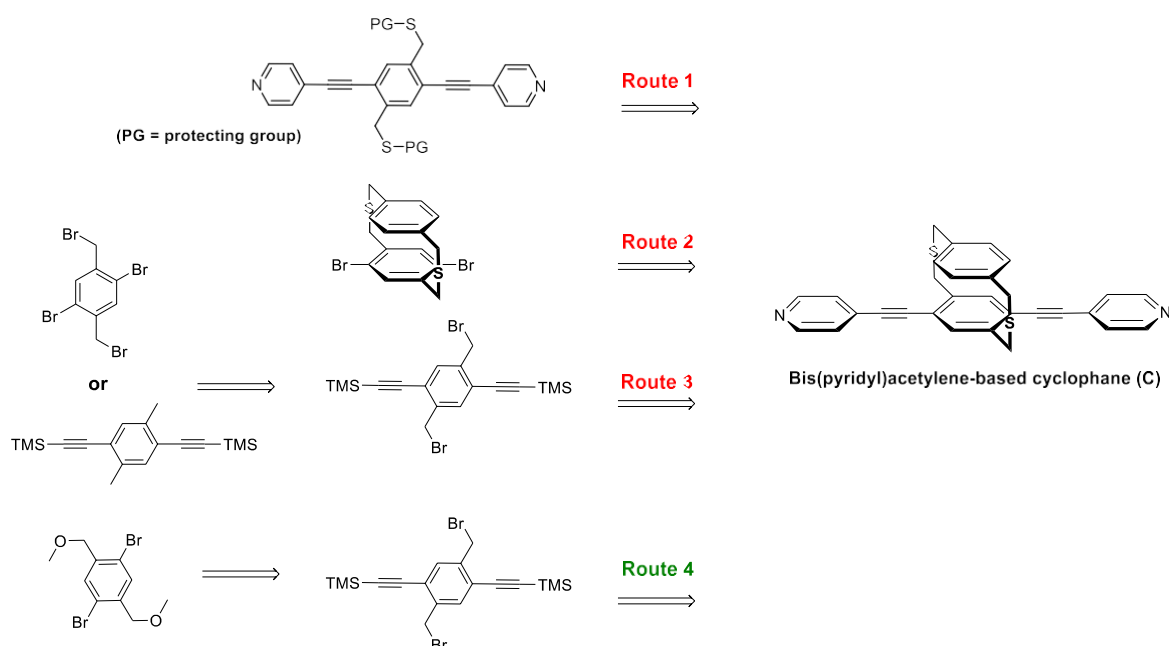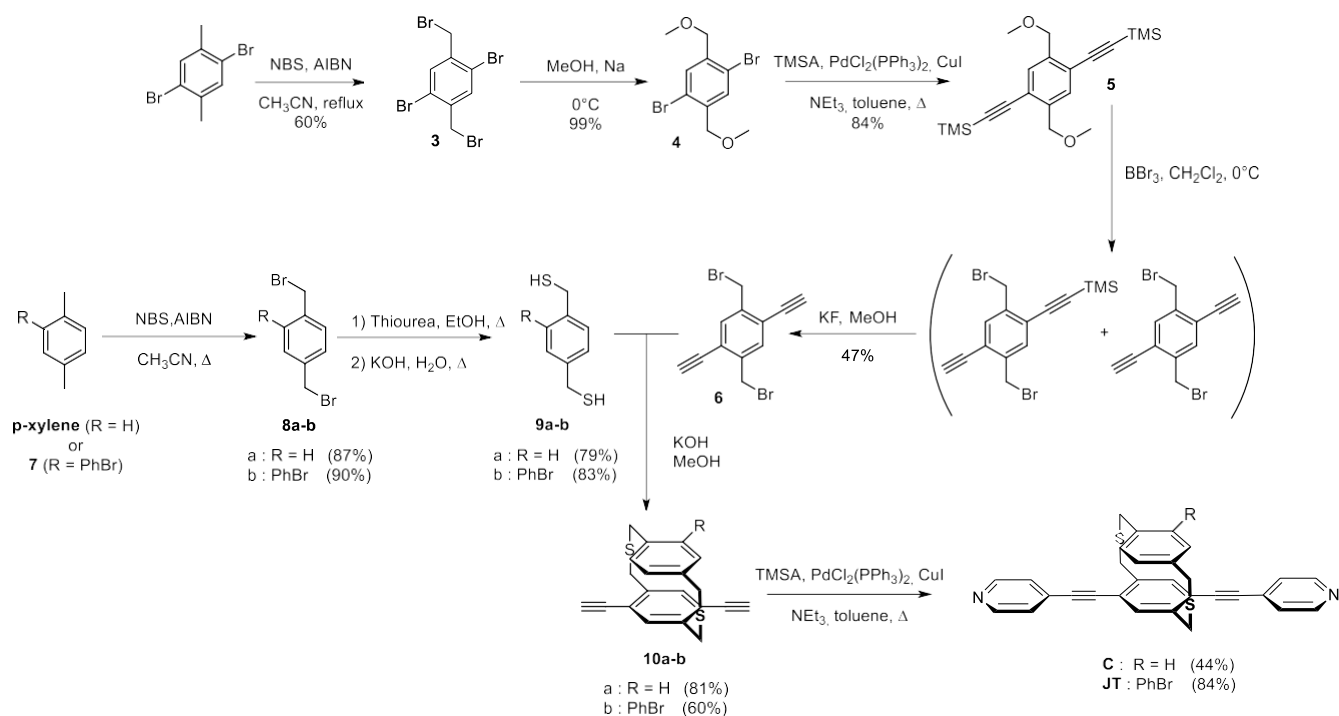

Scheme 2: Synthesis of **P**

The syntheses of the cyclophane derivatives **C** and **JT** were not as simple and therefore several retrosynthetic routes were pursued in order to finally obtain the desired compounds (scheme 3). A total of four approaches were investigated with only route number four resulting successful (scheme 4).

Following route 4, 1,4-dibromo-p-xylene was brominated with NBS, following the Wohl and Ziegler radical pathway where AIBN is the radical initiator.[16] The two bromomethyl groups of **3** were then protected by methoxy units (**4**) in order to perform a Sonogashira coupling with TMSA and give intermediate **5**. After deprotection of both methoxy and trimethylsilyl groups using boron tribromide and potassium fluoride, respectively; the resulting compound **6** and either 1,4-bis(mercaptomethyl)benzene or 1,4-bis(mercaptomethyl) -2-(*p*-bromophenyl)-benzene were solubilised in dichloromethane and slowly added to a highly diluted solution of potassium hydroxide in methanol, to afford the cyclophane derivatives.

Finally, a last Sonogashira coupling with iodopyridine enabled us to recover the final products C and JT with an overall yield of 8% and 10%, respectively.

NJC

ARTICLE

Scheme 3: Retrosynthetic routes attempted to reach target compound **C**

Scheme 4: Synthesis of **C** and **JT**

NJC

ARTICLE

It is important to note as well that the Janus tecton JT was obtain as a mixture of two structural isomers, staggered and eclipsed, which could not be separated by chromatography.

3.2 Nuclear Magnetic Resonance

All intermediates and final compounds were first studied by NMR to confirm their chemical structures, before confirming their purity by elemental analysis or high resolution mass spectrometry. As an example, the ^{1}H NMR spectrum of **C** in deuterated chloroform is depicted in Figure 1.
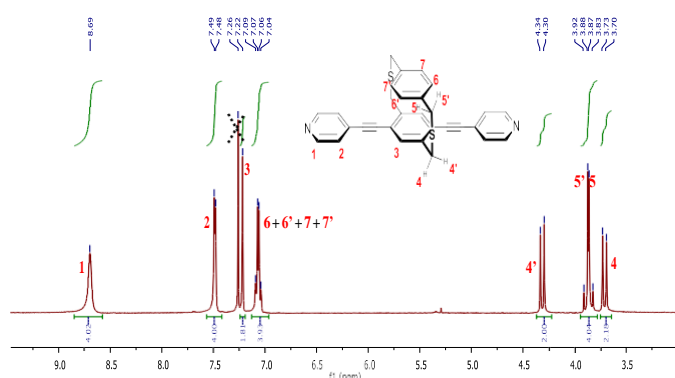
Figure 1: 300 MHz ^{1}H NMR of C in deuterated chloroform

The attribution of the aromatic part of this spectrum was made easy by the previous study of **P** pedestal's NMR spectrum. Thus, the pyridine's protons 1 and 2 respectively correspond to the wide singlet at 8.69 ppm and to the doublet at 7.48 ppm, both integrating for four protons. Then the protons 3 borne by the lower deck of the cyclophane are represented by a peak at 7.22 ppm, integrating for 2. Finally, 6, 6', 7 and 7' are attributed to the close pair of doublet with a chemical shift of 7.06 ppm integrating for 4 protons. These signals are undergoing a "roof-top effect" which indicates the second order coupling occurring between 6 and 6', and between 7 and 7'. This slight coupling might occur because in each pair, one is located above the alkyne (6 and 7') and the other above a simple proton (6' and 7). As a consequence, the deshielding of the alkyne would slightly affect one of each pair, making them lightly different. A representation of the deshielding area of the alkyne is represented in Figure 2.
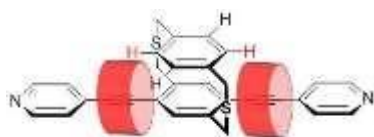
Figure 2: Deshielding effect of the alkyne unit in C

The attribution of the second part of the spectrum, concerning the CH_2 protons of the cyclophane-bridge, is entirely based on second order couplings. Four doublets with a roof-top shape can be observed at the chemical shifts of 4.32, 3.90, 3.85 and 3.70 ppm, integrating for 2 protons each. The protons 4' and 5' should thus be deshielded compared to their homologues 4 and 5. However, since 4' is closer to the alkyne than 5', the effect would be enhanced. As a consequence, 5 and 5' are respectively attributed to the pair of doublets located at 3.85 and 3.90 ppm, 5' being slightly more deshielded than 5. The protons 4 are the more shielded of all, and correspond to the doublet at 3.70 ppm. Finally 4', the most deshielded of all, is located at 4.32 ppm.

3.3 Photophysics

The absorption and emission spectra of both molecules **P** and **C** were measured in dichloromethane, as depicted in the Figure 3.
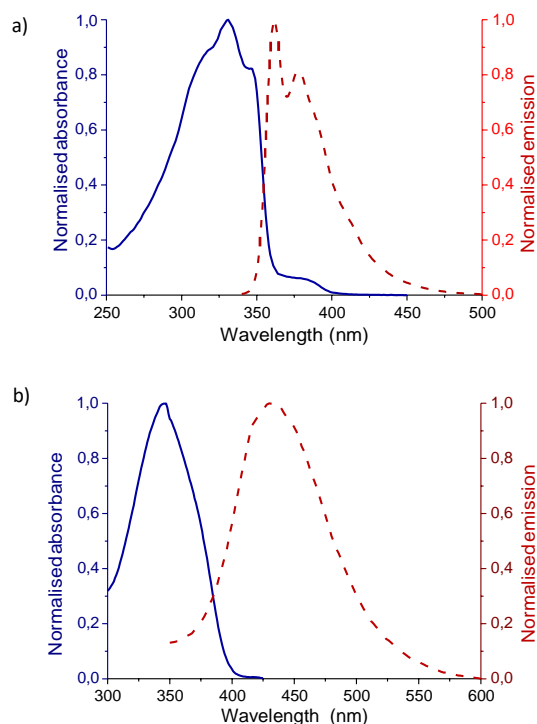
Figure 3: Absorption and emission spectra of **P** (a) and **C** (b) in dichloromethane

On the one hand, the absorption spectrum of **P** presented four transition bands at 318, 331, 347 and 380 nm, the band at λ_{max} = 331 nm being used to estimate the extinction coefficient (ε), which was calculated at 35500 $Lmol^{-1}cm^{-1}$. The emission spectrum showed

fluorescence in the blue region with a λ_{max} at 362 nm, giving a Stokes shift value of 31 nm (1100 cm^{-1}). On the other hand, molecule **C** presented one single absorption band at λ_{max} = 345 nm. The fluorescence was redshifted from **P**, emitting at λ_{max} = 434 nm with a new Stokes shift of 89 nm (5900 cm^{-1}), indicating a higher degree or reorganisation of the derivative **C**'s excited state in comparison with that of pedestal **P**.

In addition, as pyridine units are commonly used as a Lewis base in organic reactions, a pH-dependent study was therefore carried out by successive additions of trifluoroacetic acid (TFA) to a solution of **P** (respectively **C**, **JT**) in dichloromethane, each addition corresponding to 0.1 equivalents of TFA in the quartz cell. We will illustrate the results with focusing on **P** (Figure 4), as **C** and **JT** compounds behave in a similar way.

As reported, the addition of acid in the solution drastically increased the absorption band intensity at 380 nm and also reduced the two bands at 318 and 331 nm with an isobestic point located at 350 nm. In addition, with a large excess of acid a slight blueshift of the maxima from 380 to 360 nm was observed, this hypsochromic shift being attributed to the second protonation.
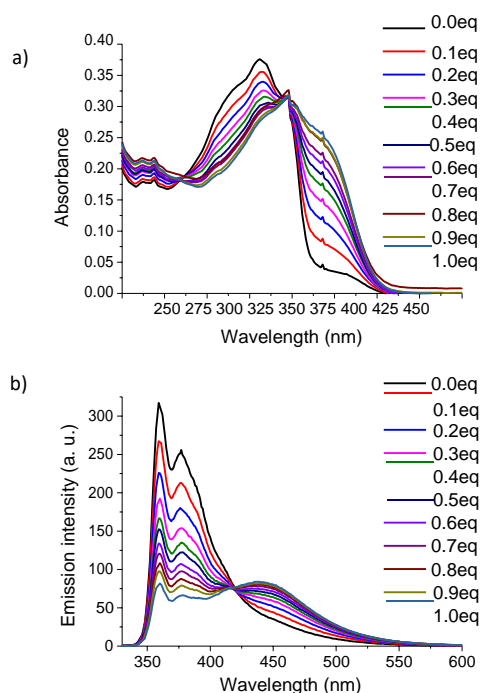

Figure 4: Absorption (a) and emission (b) spectra of **P** acidified with TFA

Moreover, the addition of acid quenched the emission of the neutral pedestal at both wavelengths 362 and 378 nm in favour of a new redshifted band at λ = 439 nm corresponding to the molecule mono-protonated. In this case, the isobestic point was located at λ = 419 nm. In accordance with the study on the absorption, a bis-protonated specie with a slight blue shift of the maxima of emission from 439 to 427 nm could be observed with a large excess of TFA. To sum up, the protonation of the pyridine units have a strong impact on the optical properties of **P**, **C** and **JT**.

3.4 Supramolecular interactions studies on bulk

Therefore, one of the aim of this work being to create self-assemblies based on the co-adsorption of **P** (respectively **C**, **JT**) with different additives, preliminary studies on bulk materials were performed, all three expected supramolecular entities being represented in Figure 5 along with the predicted supramolecular bonds with the pedestal **P**.
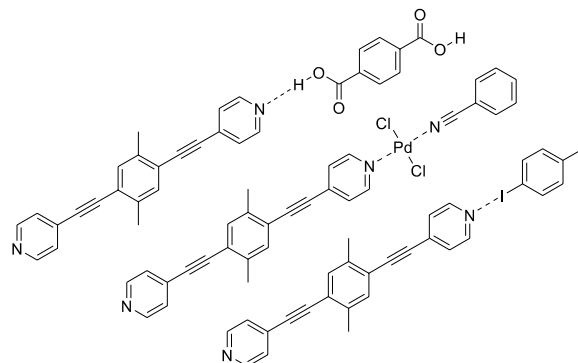

Figure 5: Expected supramolecular bonds between the pedestal **P** (respectively **C**, **JT**) and a) terephtalic acid TPA (H-bond), b) bis(benzonitrile)PdCl$_2$ Pd^{II} (coordination bond) and c) 1,4-diiodobenzene IPhI (X-bond)

As evidenced by the protonation studies, the formation of ionic bonds by **P** (respectively **C**, **JT**) could be monitored by changes in the absorption and emission spectra after adding acid in the solution. But common characterisation to measure the strength of other supramolecular bonds such as coordination, hydrogen and halogen bonding by NMR being unsuccessfull due to poor solubility, additional infrared studies were performed.

To do so, as an example, different supramolecular entities were prepared in solution by simply mixing **P** with bis(benzonitrile)-palladium(II) for coordination (**P-Pd^{II}**), terephtalic acid for hydrogen bond (**P-TPA**) and finally 1,4-diiodobenzene for halogen bond (**P-IPhI**). The infra-red spectra were recorded on bulk after evaporation or filtration of the supramolecular complexes (see Figure S29 in SI). Note that the specific C-N stretching band within the pyridine units is centered at 1591 cm^{-1} for **P** (see Figure 6), this shift being known to depend on the different supramolecular assemblies present, as described for different coordination complexes in the literature.[22]
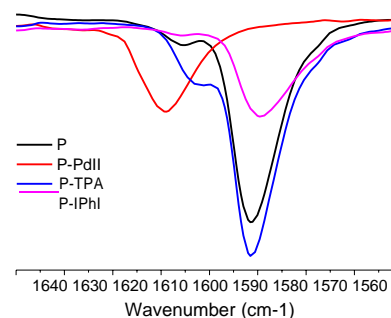

Figure 6: Infra-red spectra of the different supramolecular entities ; focus on the C-N stretching bands

The stretching bond value of the C-N bond is shifted by 18 cm^{-1} in the **P-Pd^{II}** (1609 cm^{-1}) compared to that of the **P** alone. We can thus

conclude to the effective formation of the coordination bonds.[22] However, considering the weak change of the stretching bond value in **P-IPhI** (1589 cm^{-1}), the halogen bonding is only suspected. Unfortunately, the hydrogen bond in **P-TPA** (1591 cm^{-1}) could not be observed. There are two possible explanations for this absence of shift: first, the procedure to prepare the supramolecular structure may not be efficient and thus the expected interactions was not obtained. Second, the pedestal may naturally display hydrogen bonds between the pyridine unit and the methyl group of its p-xylene core. As a consequence, the pedestal alone could already present the signal of a hydrogen bonded pyridine. This second hypothesis would be in accordance with the negative shift for the halogen bond (weaker than the H-bond) and the positive shift of the coordination bond (stronger than the H-bond).

3.5 Self-assembly of P on HOPG

Scanning tunnelling microscopy (STM) was used to observe first the self-assembly of the pedestal **P** alone at the liquid/solid interface. Indeed, based on our previous works on Janus tectons, we expect that the arrangement of C and JT would be similar on the same substrate, since in all known examples the lower-deck (pedestal, P) governs the final arrangement. This is the reason why we focused first on this model planar tecton, which is more easily imaged by STM than its 3D derivatives. Experimentally, a solution of **P** in dichloromethane was prepared at a concentration of 10^{-3} mol.L^{-1} and deposited on the HOPG surface. As shown in Figure 7 (a), ordered 2D domains formed by the assembly of pedestal **P** were observed as bright more or less elongated patterns in a quasi-square lattice network with the unit cell dimensions a = 2.1±0.1 nm, b = 2.2±0.1 nm and an angle α = 94°±2°. Figure 7 (b) shows a first set of bright patterns that are nearly parallel to the fast-scan direction. A second set of less contrasted patterns are elongated in the direction perpendicular to the former (I.e. close to the slow scan direction). These patterns can be ascribed to a quasi-square molecular lattice with two nearly-perpendicular rod-shaped molecules per unit cell as illustrated in upper left corner of figure 7 (b). Larger-scale STM images show numerous domains oriented at approximately 0°, ±30°, ±60° from each other, as illustrated in figure 7 (c). Following the principles of molecular epitaxy on HOPG, [23] these data are consistent with the model approximately described in figure 7 (d) : One axis of

the quasi-square lattice is close to a <100> axis of HOPG surface whereas the other is close to the <110> axis perpendicular to the former <100> one. Notice that this relation with HOPG is preserved through a 30° (mod. 60°) rotation of the molecular lattice, which explains the observed orientations between domains. Since the lattice is formed of two prochiral molecules in the same left- or right-handed configuration, the lattice itself is pro-chiral, and becomes chiral by considering the vertical axis orientation due to the substrate surface.[24] One thus expect the existence of mirror symmetric domains forming angles of ±θ with HOPG <100> axis.[23] From STM image and molecular model [figure 7 (c-d)] it appears that θ is small, i.e. of the order of 2°. It nevertheless explains the small variations of domain-to-domain angles with respect to the 0°, ±30°, ±60° rule. The above mentionned difference in contrast between the two molecules in the unit cell can be explained by the difference of relations between molecule and HOPG conjugated orbitals which is known to strongly influence the electron density of states.[25] An influence of tip shape cannot be ruled out, and can also contribute to this differential contrast and more specifically to the different patterns presented by the same molecules with different orientations.

Considering the organised system absorbed on the surface, the network seems to be driven by hydrogen bonds between the pyridine units and the methyl groups on the core of the molecule. This is consistent with the principles of interactions between adsorbed molecules with pyridyl and alkyl terminations.[15] Such pyridyl-driven assemblies has been observed for molecules bearing two[26-28] but also three[29-31] and even four pyridine entities[32]. The proposed scheme [figure 7 (d)] is fully consistent with the assembly of short bivalent pyridyl-terminated rod-shaped molecules [FC5]. Notice however, that longer molecules could lead to structures with parallel molecules in order to improve the coverage.[27] The observation that the same molecular arrangement can align either on a <100> or <110> direction of HOPG shows the poor influence of the substrate on the organization. This is further substantiated by the above cited literature which shows that the same self-assembling principles apply for various substrates as dissimilar as Au and HOPG. This self-assembly thus appears to be driven by intrinsic intermolecular interactions, which doesn't need assistance of the substrate in contrast with alkyl-chain based assembly.
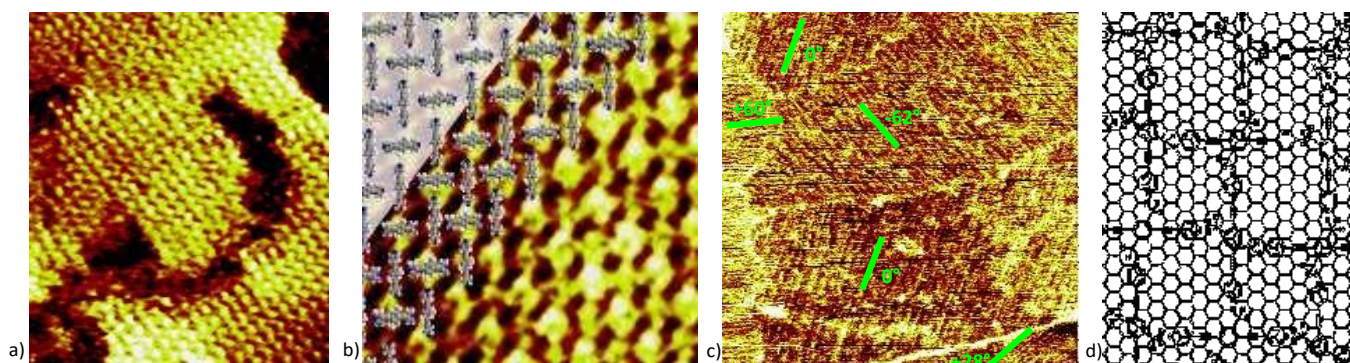

Figure 7: STM images of the self-assembled monolayer of **P** (a, I = 35 pA, U$_{bias}$ = 630 mV, 50 x 50 nm), with overlaid molecular models (b, 10 x 10 nm) large scale (c, 110nm) showing different domain orientations (light green) and the molecular model on a HOPG layer (d).

Conclusions

We designed and synthesised new molecular architectures based on the 3D Janus tecton concept that can be suitable for surface self-assembly by supramolecular interactions such as ionic, coordination, halogen or hydrogen bonding. These non-covalent interactions were studied by pH-dependent absorption and emission measurements, and by infra-red spectrometry which proved that both ionic and coordination bonding are compatible with the molecules' design. Finally, the supramolecular self-assembly of the pedestal **P** was studied on HOPG at the liquid/solid interface. The arrangement of the molecules on HOPG show a quasi-square lattice formed by hydrogen bonding between the pyridine unit and the methyl groups on the *p*-xylene core. The quasi-square lattice indicates strong intermolecular interactions are present between the **P** molecules leading to a supramolecular self-assembly which is independent of the underlying HOPG structure. As perspectives, such different interactions being able to favour or modify the supramolecular self-assembly of **P** (respectively **C**, **JT**) at the liquid/solid interface, additional experiments will be performed in a near future to study their different supramolecular self-assemblies with other substrates.

Conflicts of interest

There are no conflicts to declare.

Acknowledgements_r

Notes and references

[1] J.V. Barth, G. Costantini and K. Kern, *Nature* 2005, **437**, 671–679.

[2] S. De Feyter and F.C. De Schryver. *J. Phys. Chem. B,* 2005, **109**, 4290–4302.

[3] D.P. Goronzy, M. Ebrahimi, F. Rosei, A.Y. Fang, S. De Feyter, S.L. Tait, C. Wang, P.H. Beton, A.T.S. Wee, P.S. Weiss and D.F. Perepichka, *ACS Nano* 2018, **12**, 7445–7481.

[4] S. Xu, Q. Zeng, J. Lu, C. Wang, L. Wan and C.L. Bai, *Surf. Sci.* 2003, **538**, L451–L459; D. Bléger, D. Kreher, F. Mathevet, A-J. Attias, G. Schull, A. Huard, L. Douillard, C. Fiorini-Debuischert and F. Charra, *Angew. Chemie - Int. Ed.* 2007, **46**, 7404–7407; G. Schull, L. Douillard, C. Fiorini-Debuisschert, F. Charra, F. Mathevet, D. Kreher and A-J. Attias, J. *Nano Lett.* 2006, **6**, 1360–1363.

[5] M.E. Stawasz, D.L. Sampson and B.A. Parkinson, *Langmuir* 2000, **16**, 2326–2342.

[6] G. Velpula, M. Li, Y. Hu, Y. Zagranyarski, W. Pisula, K. Muellen, K.S. Mali and S. De Feyter, *Chem. Eur. J.* 2018, **24**, 12071 – 12077 ; O.D. Arado, M. Luft, H. Mönig, P.A. Held, A.; Studer, S. Amirjalayer and H. Fuchs, *Phys. Chem. Chem. Phys.* 2016, **18**, 27390–27395; S. Stepanow, T. Strunskus, M. Lingenfelder, A. Dmitriev, H. Spillmann, N. Lin, J.V. Barth, C. Wöll and K. Kern, *J. Phys. Chem. B* 2004, **108**, 19392–19397; M. Ruiz-Osés, T. Kampen, N. González-Lakunza, I. Silanes, P.M. Schmidt-Weber, A. Gourdon, A. Arnau, K. Horn and J.E. Ortega, *ChemPhysChem* 2007, **8**, 1722–1726.

[7] K-H. Chung, J. Park, K.Y. Kim, J.K. Yoon, H. Kim, S. Han and S.J. Kahng, *Chem. Commun.* 2011, **47**, 11492-11494; R. Gutzler, H. Walch, G. Eder, S. Kloft, W.M. Heckl and M. Lackinger, *Chem. Commun.* 2009,

29, 4456–4458; J.C. Russell, M.O. Blunt, J.M. Garfitt, D.J. Scurr, M. Alexander, N.R. Champness and P.H. Beton, *J. Am. Chem. Soc.* 2011, **133**, 4220–4223.

[8] B. Song, S. Kandapal, J. Gu, K. Zhang, A. Reese, Y. Ying, L. Wang, H. Wang, Y. Li, M. Wang, S. Lu, X-Q. Hao, X. Li, B. Xu and X. Li, *Nat. Comm.* 2018, **9**, 4575 ; N. Lin, A. Langner, S.L. Tait, C. Rajadurai, M. Ruben and K. Kern, *Chem. Commun.* 2007, **1**, 4860-4862; M.A. Lingenfelder, H. Spillmann, A. Dmitriev, S. Stepanow, N. Lin, J.V. Barth and K. Kern, *Chem. - A Eur. J.* 2004, **10**, 1913–1919; S. Stepanow, M. Lingenfelder, A. Dmitriev, H. Spillmann, E. Delvigne, N. Lin, X. Deng, C. Cai, J.V. Barth and K. Kern, *Nat. Mater.* 2004, **3**, 229–233.

[9] L. Sosa-Vargas, E. Kim and A-J. Attias, *Mater. Horiz.*, 2017, **4**, 570; K. Ariga, M. Nishikawa, T. Mori, J. Takeya, L.K. Shrestha and J.P. Hill, *Sci. Tech. Adv. Mater*. 2019, **20:1**, 51-95.

[10] Z.C. Dong, X.L. Zhang, H.Y. Gao, Y. Luo, C. Zhang, L.G. Chen, R. Zhang, X. Tao, Y. Zhang, J.L. Yang and J.G. Hou, *Nat. Photonics* 2010, **4**, 50–54.

[11] X.H. Qiu, *Science* 2003, **299**, 542–546; J. Repp, G. Meyer, S.M. Stojković, A. Gourdon and C. Joachim, *Phys. Rev. Lett.* 2005, **94**, 26803.

[12] J.A. Mann, J. Rodríguez-López, H.D. Abruña and W.R. Dichtel, *J. Am. Chem. Soc.* 2011, **133**, 17614–17617.

[13] P. Du, M. Jaouen, A. Bocheux, C. Bourgogne, Z. Han, V. Bouchiat, D. Kreher, F. Mathevet, C. Fiorini-Debuisschert, F. Charra and A-J. Attias, *Angew. Chemie Int. Ed.* 2014, **5**, 10060–10066.

[14] S. Le Liepvre, P. Du, D. Kreher, F. Mathevet, A-J. Attias, C. Fiorini-Debuisschert, L. Douillard and F. Charra, *ACS Photonics* 2016, **3**, 2291–2296.

[15] X. K. Li, S. Q. Zhang, J. Q. Li, Y. X. Qian, W. B. Duan and Q. D. Zeng, *New Journal of Chemistry,* 2019, **43,** 13315-13325

[16] S. Takahashi, Y. Kuroyama, K. Sonogashira and N. Hagihara, *Synthesis (Stuttg.)* 1980, 627–630.

[17] L. A. Carpino and A.C. Sau, *J. Chem. Soc., Chem. Commun.* 1979, **11**, 514–515.

[18] K. Sonogashira, Y. Tohda and N. Hagihara, *Tetrahedron Lett.* 1975, **16**, 4467–4470.

[19] C. Djerassi, *Chem. Rev.* 1948, **43,** 271–317.

[20] H.R. Hudson, R.R.F. Kinghorn and W.S. Murphy, *J. Chem. Soc. C.* 1971, 3593-3596.

[21] G.W. Stacy, A.J. Papa, F.W. Villaescusa and S.C. Ray, *J. Org. Chem.* 1964, **29** (3), 607–612.

[22] I.S. Perelygin and M.A. Klimchuk, *J. Appl. Spectrosc.* 1976, **24** (1), 43–46.

[23] D. Bleger, D. Kreher, F. Mathevet, A. J. Attias, I. Arfaoui, G. Metge, L. Douillard, C. Fiorini-Debuisschert and F. Charra, *Angewandte Chemie-International Edition,* 2008, **47,** 8412-8415.

[24] N. Katsonis, E. Lacaze and B. L. Feringa, *Journal of Materials Chemistry,* 2008, **18,** 2065-2073.

[25] N. Kalashnyk, M. Jaouen, C. Fiorini-Debuisschert, L. Douillard, A. J. Attias and F. Charra, *Chemical Communications,* 2018, **54,** 9607-9610.

[26] M. A. Dubois, O. Guillermet, S. Gauthier, G. Zhan, Y. Makoudi, F. Palmino, X. Bouju and A. Rochefort, *Physical Chemistry Chemical Physics,* 2018, **20,** 15350-15357.

[27] D. Hotger, P. Carro, R. Gutzler, B. Wurster, R. Chandrasekar, S. Klyatskaya, M. Ruben, R. C. Salvarezza, K. Kern and D. Grumelli, *Physical Chemistry Chemical Physics,* 2018, **20,** 15960-15969.

[28] M. El Garah, A. Ciesielski, N. Marets, V. Bulach, M. W. Hosseini and P. Samori, *Chemical Communications,* 2014, **50,** 12250-12253.

[29] A. Mukherjee, J. Teyssandier, G. Hennrich, S. De Feyter and K. S. Mali, *Chemical Science,* 2017, **8,** 3759-3769.

30 T. R. Umbach, M. Bernien, C. F. Hermanns, L. L. Sun, H. Mohrmann, K. E. Hermann, A. Kruger, N. Krane, Z. Yang, F. Nickel, Y. M. Chang, K. J. Franke, J. I. Pascual and W. Kuch, *Physical Review B,* 2014, **89,** 235409.

31 A. Ciesielski, P. J. Szabelski, W. Rzysko, A. Cadeddu, T. R. Cook, P. J. Stang and P. Samori, *Journal of the American Chemical Society,* 2013, **135,** 6942-6950.

32 A. Stein, D. Rolf, C. Lotze, C. Czekelius, K. J. Franke and P. Tegeder, *Journal of Physics-Condensed Matter,* 2019, **31**, 044002.